

# Identification of Nuclear Relaxation Processes in a Gapped Quantum Magnet: $^1\text{H}$ NMR in the $S = \frac{1}{2}$ Heisenberg Ladder $\text{Cu}_2(\text{C}_5\text{H}_{12}\text{N}_2)_2\text{Cl}_4$

G. Chaboussant<sup>1</sup>, M.-H. Julien<sup>1</sup>, Y. Fagot-Revurat<sup>1</sup>, L.P. Lévy<sup>1,2</sup>, C. Berthier<sup>1,3</sup>, M. Horvatić<sup>1</sup> and O. Piovesana<sup>4</sup>

<sup>1</sup>Grenoble High Magnetic Field Laboratory, CNRS and MPI-KFK, BP 166, F-38042 Grenoble Cedex 9, France

<sup>2</sup>Institut Universitaire de France and Université J. Fourier, BP 41, F-38400 St. Martin d'Hères, France

<sup>3</sup>Laboratoire de Spectrométrie Physique, Université J. Fourier, BP 87, F-38402 St. Martin d'Hères, France

<sup>4</sup>Dipartimento di Chimica, Università di Perugia, I-06100 Perugia, Italy

(October 23, 2018)

The  $^1\text{H}$  hyperfine shift  $K$  and NMR relaxation rate  $T_1^{-1}$  have been measured as a function of temperature in the  $S = 1/2$  Heisenberg antiferromagnetic ladder  $\text{Cu}_2(\text{C}_5\text{H}_{12}\text{N}_2)_2\text{Cl}_4$ . The presence of a spin gap  $\Delta \simeq J_\perp - J_\parallel$  in this strongly coupled ladder ( $J_\parallel < J_\perp$ ) is supported by the  $K$  and  $T_1^{-1}$  results. By comparing  $T_1^{-1}$  at two different  $^1\text{H}$  sites, we infer the evolution of the spectral functions  $S_z(q, \omega_n)$  and  $S_\perp(q, \omega_n)$ . When the gap is significantly reduced by the magnetic field, two different channels of nuclear relaxation, specific to gapped antiferromagnets, are identified and are in agreement with theoretical predictions.

Several classes of one-dimensional Heisenberg antiferromagnets (HAF) are known to exhibit a spin-gap at low temperature. For example, integer-spin chains [1] have a non-magnetic "spin-liquid" ground state (singlet) separated from a branch of triplet excitations by an energy gap  $\Delta$ . A spin-liquid ground state also exists in spin-ladders, built by coupling an even number of  $S = 1/2$  HAF chains with an antiferromagnetic transverse exchange  $J_\perp$  [2,3]. At low energies, many physical properties are dominated by the singlet-triplet gap and do not depend on the underlying dynamical quantum processes stabilizing the ground state. For example, thermodynamic quantities (susceptibility, specific heat) are very similar in a number of gapped one-dimensional HAF.

In this letter, the low-energy dynamical processes dominating the  $^1\text{H}$  spin-lattice relaxation rate ( $1/T_1$ ) of an organic spin-ladder ( $\text{Cu}_2(\text{C}_5\text{H}_{12}\text{N}_2)_2\text{Cl}_4$ ) are unambiguously identified by comparing the  $T_1$  measurements at two proton sites. They coincide precisely with the processes proposed by Sagi and Affleck [4] for Haldane systems. This experimental evidence supports the idea proposed by Sachdev and coworkers [5] that spectral functions  $S_{z,\perp}(q, \omega)$  are, at low energies ( $\omega \ll \Delta$ ), common to all gapped one-dimensional HAF.

In  $\text{Cu}_2(\text{C}_5\text{H}_{12}\text{N}_2)_2\text{Cl}_4$  [6], the  $\text{Cu}^{2+}$  ( $S=1/2$ ) ions are coupled antiferromagnetically in *well isolated* ladders [7] (see Fig. 1). The exchange parameters along the rungs ( $J_\perp$ ) and the legs ( $J_\parallel$ ) of the ladder are isotropic and have been accurately measured to be  $J_\perp = 13.2$  K and  $J_\parallel = 2.4$  K [8–10]. In many respects, this material is a model system in which theoretical predictions for Heisenberg ladders in the strong coupling limit ( $J_\perp/J_\parallel \equiv 5.5 \gg 1$ ) can be tested.

The  $^1\text{H}$  NMR measurements were carried out by pulsed spin-echo techniques on five single crystals (typically  $1 \times 1 \times 0.05$  mm<sup>3</sup>), oriented with their  $\hat{b}$  axis (perpendic-

ular to the chains axes) along the applied field  $H_0 = 5.6$  Tesla. A typical spectrum for the proton resonance shows a number of partially resolved lines (Fig. 2a), indicating a variety of local fields among the 24 inequivalent  $^1\text{H}$  sites. In the following, we focus on the lines labelled (I) and (II), as their extreme position in the spectrum allows their study on a wide temperature ( $T$ ) range [11]. With the field along  $\hat{b}$ , the magnetic hyperfine shift  $K_{bb}$  of the proton resonance is related to the uniform spin susceptibility  $\chi_0 = \chi_i(q=0, \omega=0)$  at the nuclear site  $i$ , by

$$K_{bb}(T) = \frac{A_{bb}}{g_{bb}\mu_B} \chi_0(T) + \sigma, \quad (1)$$

where  $A_{bb}$  is the hyperfine coupling constant and  $\sigma$  the chemical shift. The shift of the two lines, plotted in Fig. 2b, are opposite in sign but follows the same  $T$ -dependence as  $\chi_0$ , that is, a high temperature Curie-Weiss behavior followed by an exponential drop below a rounded maximum at  $T_{\chi_{max}} \simeq 8$  K, in complete agreement with previous susceptibility measurements [8,10]. Since  $K$  is proportional to the susceptibility  $\chi_0$  measured at 5 T (Inset to Fig. 2b), the hyperfine couplings on both sites can be estimated:  $A_{bb}^{(I)} = +2.95 \pm 0.40$  kOe and  $A_{bb}^{(II)} = -2.6 \pm 0.50$  kOe [12]. The largest contribution to  $A$  comes from the dipolar field on the  $j$ -th nucleus created by the surrounding electronic spins, i.e.  $A_j \propto -|\gamma_e|\gamma_n\hbar^2 \sum_i (1 - 3\cos^2\theta_{ij})/r_{ij}^3$ , where  $\theta_{ij}$  is the angle between  $r_{ij}$  and  $H_0$ . Given the atomic positions, it is straightforward to compute the dipolar field at each  $^1\text{H}$  site (a reliable result is obtained by summing over 5-6 neighboring Cu spins). The total NMR spectrum is well-reproduced in this way. It is therefore possible to assign the NMR lines to specific proton sites: line (II) is ascribed to protons H2 involved in the superexchange  $J_\parallel$  (See Fig. 1). The line (I) is attributed to protons

H20 and H23 at the outer edges of the ethyl groups. It must be stressed that the uncertainty in the site labelling could only result in adding the protons H14 and H4 to the lines (I) and (II), respectively. This essentially does not affect our analysis of the nuclear relaxation.

In a magnetic field, the triplet excitations split into three branches. In the strong coupling limit ( $J_{\parallel}/J_{\perp} \ll 1$ ), the lowest branch is separated from the singlet ground state by an effective gap  $\Delta_h = \Delta - h$ , where  $h = g\mu_B H_0$  is the Zeeman energy. When the temperature is small compared to  $\Delta_h$ , interactions between excitations are negligible and the lowest branch dominates the temperature dependence of the susceptibility [13]

$$\chi_0 \propto \frac{1}{\sqrt{k_B T J_{\parallel}}} \exp\left(-\frac{\Delta_h}{k_B T}\right). \quad (2)$$

A low temperature fit of  $K^{(I)}$  to Eq. (1) and (2) gives an effective gap of  $\Delta_h \simeq 3$  K in 5.6 Tesla. This is very close to the value expected taking the zero-field gap  $\Delta = 10.8$  K inferred from susceptibility and high field magnetization measurement [8] reduced by the Zeeman energy  $h = 7.6$  K. Thus, the measurements of  $K$  and  $\chi_0$  are fully consistent with a spin gap  $\Delta_h = (J_{\perp} - J_{\parallel}) - h$  between the singlet and triplet states of the Heisenberg ladder with strong rungs.

We now discuss the dynamical properties, as probed by the nuclear spin-lattice relaxation rate  $1/T_1$ . The recovery of the nuclear magnetization is always a single exponential at all temperatures. As shown in Fig. 3a, both sites display qualitatively the same  $T$ -dependence, that is,  $1/T_1$  tends to be constant in the paramagnetic region, and crosses over to an activated behavior at low  $T$ . There are, however, striking differences between the two lines: (a) at high- $T$  the values of  $T_1$  differ by one order of magnitude, (b) at low- $T$  the gap values differ by a factor of 2. Indeed, assuming an activated behavior  $1/T_1 \propto \exp(-\Delta_{eff}/k_B T)$ ,  $\Delta_{eff} \simeq 3.4 \pm 0.2$  K for the line (I), close to the value  $\Delta_h = 3.0$  K deduced from the shift, but  $\Delta_{eff} \simeq 6.8 \pm 0.2$  K for the line (II).

In spin systems, the temporal fluctuations of the electronic spins make the nuclear polarization relax in a time  $T_1$  related to the spectral densities  $S_{z,\pm}(q, \omega)$  of the two-spin correlation functions, through [14]

$$\frac{1}{T_1} = \frac{(\gamma_n \gamma_e \hbar)^2}{2} \sum_q [F_z S_z(q, \omega_n) + F_{\perp} S_{\perp}(q, \omega_n)], \quad (3)$$

with  $\omega_n \sim 0$  the nuclear Larmor frequency, and

$$S_{z,\pm}(q, \omega_n) = \int dt e^{i\omega_n t} \langle \{S_{z,+}(q, t) S_{z,-}(-q, 0)\} \rangle. \quad (4)$$

In general, any quantitative analysis of the relaxation requires the knowledge of the hyperfine "form" factors  $F(q)$  [15] in addition to a model for  $S_{z,\pm}(q, \omega)$ . We first discuss the structure factors  $S_{z,\pm}(q, \omega)$ .

Single magnon processes, which require an energy greater or equal to the gap, cannot contribute to the nuclear relaxation which involves negligible energy transfers  $\hbar\omega_n \sim mK$ . Two- or three-magnon scattering processes are then required [16]. More specifically, Sagi and Affleck [4] have recently analyzed the possible nuclear relaxation processes for Haldane chains in magnetic fields. Since the low energy excitations of  $S = 1/2$  ladders and integer-spin chains are qualitatively similar [17], it is natural to consider the same processes here. Following their arguments, the nuclear spins can exchange energy through three different channels [4]:

- (i) "intra-branch" transitions involve two magnons within the same branch (i.e. with the same  $S_z$  eigenvalue). At low  $T$ , these processes have a maximum probability near the minimum at  $k = \pi$  of the lowest branch of the triplet (Fig. 4), implying a momentum transfer  $\Delta k = q \sim 0$  (forward scattering). For  $T \ll h$ , the  $q$ -integrated spectral density is expected to follow the thermal occupation of the lowest energy triplets  $S_z^{intra}(\omega_n) \propto \exp(-(\Delta - h)/k_B T)$ .

- (ii) "inter-branch" transitions (Fig. 4), *i.e.* transitions from a state in a magnon branch  $m$  to a state with  $m \pm 1$  ( $S_{\pm}$  operators). Since the Zeeman splitting at 5.6 Tesla is larger than the magnon bandwidth ( $\sim 5.5$  K [18]), these processes can only occur because of the finite damping of each level and are expected to be weak. Furthermore, only large momentum transfers  $q \sim \pi$  (backward scattering) remain at large Zeeman splitting. One infers from [4] that  $S_{\perp}^{inter}(\omega_n) \propto \exp(-\Delta/k_B T)$ .

- (iii) "staggered" processes: when  $H_0$  approaches the critical field  $h_{c1} \approx \Delta$ , one-magnon excitations ( $S_{\pm}$  operators,  $q \sim \pi$ ) become increasingly relevant. At finite  $T$  in the gapped phase, interactions between excitations, or equivalently finite damping, generate non-vanishing matrix elements for such transitions: this relaxation mechanism involves three-magnon (or higher order) processes, and its temperature dependence follows the square of the thermal population in the lowest triplet state,  $S_{\perp}^{stagg}(\omega_n) \propto \exp(-2(\Delta - h)/(k_B T))$ .

The above discussion shows that: (1) the Boltzmann factor is more favorable to intra-branch processes ( $\Delta_h \simeq 3$  K); these will dominate the staggered transitions ( $2\Delta_h \simeq 6$  K), while inter-branch ones, if any, are essentially negligible ( $\Delta \simeq 10$  K). (2) The low- $T$  nuclear relaxation is only driven by two terms:  $S_z(q \sim 0, \omega_n)$  for intra-branch transitions and  $S_{\perp}(q \sim \pi, \omega_n)$  for staggered transitions. Accordingly, we write Eq. (3) in a simplified form:

$$1/T_1 \propto F_z(0) S_z(q = 0, \omega_n) + F_{\perp}(\pi) S_{\perp}(q = \pi, \omega_n). \quad (5)$$

Hence, the two behaviors  $1/T_1 \propto \exp(-\Delta_h/k_B T)$  for the line (I) and  $1/T_1 \propto \exp(-2\Delta_h/k_B T)$  for (II) can only come from the temperature dependence of  $S_z(q = 0, \omega_n) \propto \exp(-\Delta_h/k_B T)$  while  $S_{\perp}(q = \pi, \omega_n) \propto \exp(-2\Delta_h/k_B T)$ . In other words, the ratio of

$F_z(0)/F_\perp(\pi)$  for lines (I) and (II) are such that, at low temperatures, only one of the exponential terms dominates the relaxation: obviously,  $S_z(q=0, \omega_n)$  component is favored for the line (I), and  $S_\perp(q=\pi, \omega_n)$  one for the line (II).

This result is, to our knowledge, the first experimental identification of specific nuclear relaxation channels in a gapped antiferromagnet, a result in remarkable agreement with the work of Sagi and Affleck. Another support to this theory is that the lowest gap  $\Delta_h \simeq 3$  K is also the value seen in the susceptibility. Furthermore, the observation of the staggered contribution in the gapped phase proves that interactions between fermionic-like excitations are significant in this system. This conclusion was already drawn from magnetization measurements [8].

A nice feature of this study is that the  $T_1$  data for the two lines provide a set of two independent equations (*i.e.* Eq. 5 for each line). Since  $F_z(q)$  and  $F_\perp(q)$  can be computed for each  $^1\text{H}$  site, the spectral functions  $S_z$  and  $S_\perp$  can, in principle, be extracted separately. Here, we found that  $F_\perp(q=\pi)$  is indeed five times larger than  $F_z(q=0)$  for the line (II), while both terms are comparable for the line (I).  $S_\perp \propto \exp(-2\Delta_h/k_B T)$  is thus *overweighted* for the line (II) explaining why  $T_1^{II}$  decays with an activation energy  $2\Delta_h$ . On the other hand,  $T_1^I$  is predominantly sensitive to the smallest gap,  $\Delta_h$ , generated by  $S_z(q=0, \omega_n)$ . However, one must realize that the calculation of the form factors is subject to several uncertainties: any error in atomic positions is amplified ( $F(r_{ij}) \propto r_{ij}^{-6}$ ), the spatial extension of  $\text{Cu}^{2+}$  orbitals may play an important role [19] for the protons H2 (line II) which are in the superexchange pathway and closer to the Cu ion than those of line (I). Indeed, the extracted values of  $S_z$  are slightly negative suggesting that the value of  $F_\perp^{II}$  has been underestimated in the calculation. In fact, the pure Heisenberg paramagnetic limit  $S_z(q, \omega_n) = \frac{1}{2}S_\perp(q, \omega_n)$  should be recovered when  $T$  is large compared to  $J_{\perp, \parallel}$  and  $h$ .  $F_\perp^{II}$  can be rescaled to a value satisfying this limit at  $T = 30$  K, where the observed value of  $T_1$  for the line (I) is within 10 % of the paramagnetic limit calculated by Moriya [14]. In any event, this rescaling does not affect the gap parameters extracted from the low- $T$  behaviour. As shown in Fig. 3c,  $S_\perp$  experiences a gap  $\Delta \simeq 6.8 \pm 0.2$  K *twice* as large as in  $S_z$  ( $3.4 \pm 0.2$  K).

This analysis of the nuclear relaxation in  $\text{Cu}_2(\text{C}_5\text{H}_{12}\text{N}_2)_2\text{Cl}_4$ , a strongly coupled ladder, settles an ongoing controversy: the gap values derived from static ( $\chi_0$ ) and dynamic  $S_z(q \sim 0, \omega_n)$  measurements are here *identical*, in complete agreement with the predictions of Troyer *et al.* [13] and Sagi and Affleck [4]. This strongly contrasts with the experimental observations in inorganic ladders [20,21], and in some Haldane chains [22,23]. In these materials, the different temperature dependence observed in the dynamics may be due to a second minimum in the dispersion relation. For exam-

ple, it should be the case in  $\text{SrCu}_2\text{O}_3$  if  $J_\perp < J_\parallel$  [24,25]. Low-lying excitations near  $k=0$  such that  $\Delta_{k=0} \sim \Delta_{k=\pi}$  may open up relaxation channels involving large- $q$  inter-branch transitions and would lead to a higher effective gap in  $T_1$  measurements. Other explanations have been proposed in the limits  $T \ll \Delta_h$  [26] and  $J_\perp \ll J_\parallel$  [27].

In conclusion,  $^1\text{H}$  NMR experiments demonstrate that the effective gap of the  $S = 1/2$  HAF ladder  $\text{Cu}_2(\text{C}_5\text{H}_{12}\text{N}_2)_2\text{Cl}_4$  in a magnetic field  $h$  is  $\Delta_h \simeq J_\perp - J_\parallel - h$ . The nuclear relaxation can be quantitatively understood in the framework of the theory of Sagi and Affleck, retaining only "intra-branch" and "staggered" processes. More generally, the processes identified in this work should be generic to many gapped HAF chains in a magnetic field.

We thank J.-P. Boucher, K. Damle and S. Sachdev for useful discussions. The GHMFL is Laboratoire Conventio-  
tionné aux Universités J. Fourier et INPG Grenoble I.

- 
- [1] F.D.M. Haldane, Phys. Rev. Lett. **50**, 1163 (1983).
  - [2] E. Dagotto, J. Riera and D.J. Scalapino, Phys. Rev. B **45**, 5744 (1992).
  - [3] E. Dagotto and T.M. Rice, Science **272**, 618 (1996).
  - [4] J. Sagi and I. Affleck, Phys. Rev. B **53**, 9188 (1996).
  - [5] S. Sachdev, T. Senthil and R. Shankar, Phys. Rev. B **50**, 258 (1994).
  - [6] B. Chiari *et al.*, Inorg. Chem. **29**, 1172 (1990).
  - [7] As to the effects of inter-ladder couplings, see M. Troyer, M.E. Zhitomirsky and K. Ueda, Phys. Rev. B **55**, R6117 (1997) and references therein.
  - [8] G. Chaboussant *et al.*, Phys. Rev. B **55**, 3046 (1997).
  - [9] C.A. Hayward, D. Poilblanc and L.P. Lévy, Phys. Rev. B, **54**, R12649 (1996); Z. Weihong, R.R.P. Singh and J. Oitmaa, Phys. Rev. B **55**, 8052 (1997).
  - [10] See also P.R. Hammar and D.H. Reich, J. Appl. Phys. **79**, 5392 (1996).
  - [11] The line (I) appears as an edge of a broad resonance. This, however, did not affect seriously relaxation measurements as  $T_1$  changes very weakly with position in this part of the spectrum and narrow frequency excitations were used.
  - [12]  $\sigma$  being  $T$ -independent can be estimated as the zero-intercept in a  $K$  vs.  $\chi_0$  plot: we find  $\sigma \simeq 0$ .
  - [13] M. Troyer, H. Tsunetsugu and D. Würtz, Phys. Rev. B **50**, 13515 (1994).
  - [14] T. Moriya, Prog. Theor. Phys. **16**, 23 (1956).
  - [15] An exact expression of  $F_z$  and  $F_\perp$  is given by: L.S.J.M. Henkens, T.O. Klaassen and N.J. Poulis, Physica (Amsterdam) **94B**, 27 (1978), and references therein.
  - [16] D. Beeman and P. Pincus, Phys. Rev. **166**, 359 (1968).
  - [17] S.R. White, Phys. Rev. B **53**, 52 (1996).
  - [18] P.R. Hammar, D.H. Reich *et al.*, unpublished.
  - [19] J.-P. Renard, private communication.
  - [20] M. Azuma *et al.*, Phys. Rev. Lett. **73**, 3463 (1994); H.

- Iwase, M. Isobe, and H. Yasuoka, J. Phys. Soc. Jpn. **65**, 2397 (1996); S. Tsuji, K.i. Kumagai, M. Kato and Y. Koike, *ibid.* 3474 (1996).
- [21] There are evidences that  $(\text{VO})_2\text{P}_2\text{O}_7$  is *not* a simple ladder [S. Nagler, Bull. Am. Phys. Soc. **42**, 286 (1997)]. However, the gap inferred from  $T_1$  data,  $\Delta_{T_1}$ , is also twice as large as  $\Delta_{\text{shift}} \simeq 30$  K [Y. Furukawa *et al.*, J. Phys. Soc. Jpn. **65**, 2393 (1996)], which is precisely the neutron gap  $\Delta \simeq 40$  K reduced by the Zeeman energy  $g\mu_B H \simeq 10$  K. For  $^{51}\text{V}$  nuclei, only transverse fluctuations contribute to  $T_1$ , involving interbranch transitions ( $\propto \exp(-\Delta/k_B T)$ ) and staggered transitions ( $\propto \exp(-2(\Delta - h)/k_B T)$ ). Both processes always lead to an effective gap larger than  $\Delta - h$ , the lowest triplet energy.
- [22] T. Shimizu *et al.*, Phys. Rev. B **52**, R9835 (1995).
- [23] M. Takigawa *et al.*, Phys. Rev. Lett. **76**, 2173 (1996).
- [24] J. Oitmaa, R.R.P. Singh and Z. Weihong, Phys. Rev. B. **54**, 1009 (1996). The dispersion relation of the ladder is calculated for various ratios of  $J_\perp/J_\parallel$ .
- [25] D.C. Johnston, Phys. Rev. B **54**, 13009 (1996).
- [26] S. Sachdev and K. Damle, Phys. Rev. Lett. **78**, 943 (1997).
- [27] J. Kishine and H. Fukuyama, J. Phys. Soc. Jpn. **66**, 26 (1997).

FIG. 1. Schematic structure of  $\text{Cu}_2(\text{C}_5\text{H}_{12}\text{N}_2)_2\text{Cl}_4$ , with the exchange parameters determined in Ref. [8]. The labelled protons contribute to the two NMR lines used in this work to probe different dynamical functions ( $S_z$  and  $S_\perp$ , see text).

FIG. 2. (a):  $^1\text{H}$  NMR spectra at fixed frequency  $f_0 = 239.112$  MHz. The arrows indicate the two lines studied (their different amplitudes are due to different excitation conditions). The large central peak comes from protons in the NMR probe. (b): magnetic hyperfine shift for the lines (I) and (II) and susceptibility at 5 Tesla; the dashed line is a fit where the hyperfine coupling is the only adjustable parameter and temperature dependence of the susceptibility is given by Eq. 5 of Ref. [8], with  $J_\perp = 13.2$  K and  $J_\parallel = 2.5$  K. Inset: shift data vs. susceptibility, with  $T$  as an implicit parameter.

FIG. 3.  $^1\text{H}$  spin-lattice relaxation rate  $1/T_1$  for lines (I) and (II) as a function of  $T$  (a) and  $1/T$  (b). (c):  $S_z(q=0, \omega_n)$  and  $S_\perp(q=\pi, \omega_n)$  correlation functions derived from  $T_1$  results (see text for details).

FIG. 4. Schematic picture of the two-magnon scattering processes relevant to the nuclear relaxation in a system with singlet to triplet gap, in a magnetic field  $H_0$  [4]. In this experiment, the Zeeman splitting  $g\mu_B H \sim 7.6$  K is larger than the magnon bandwidth ( $\sim 5.5$  K [18]).

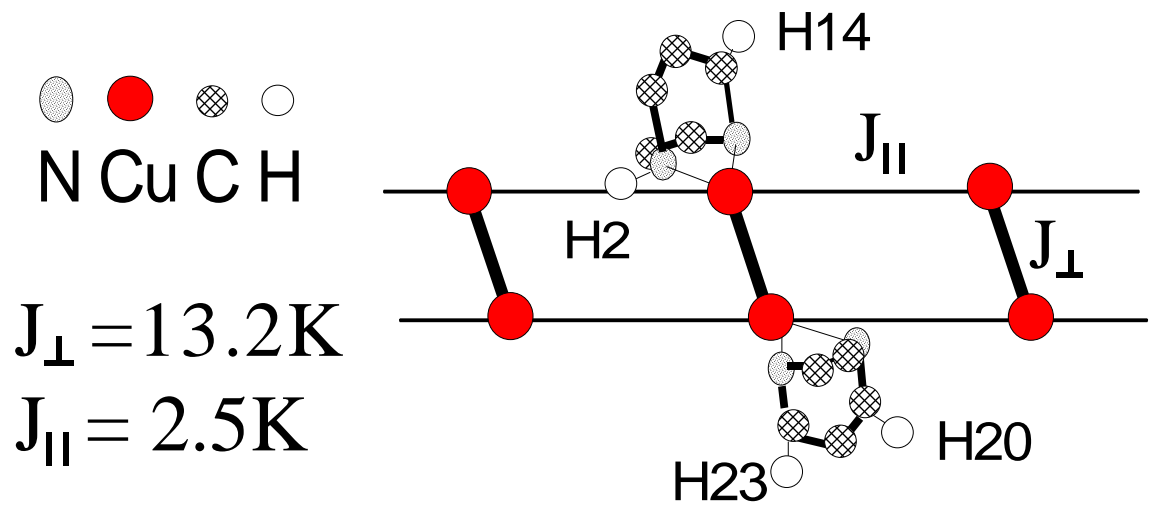


Figure 1  
Chaboussant et al

